A POSSIBLE SUBAQUEOUS HYDROTHERMAL SYSTEM IN MELAS CHASMA, MARS. J. Heidenreich, E. Rogers, B. Qualizza, H. Dawson, B. Horgan (briony@purdue.edu) [1]Earth, Atmospheric, and Planetary Sciences, Purdue University.

Introduction: Mars' Southwest Melas Chasma is located in Valles Marineris, just below the main Melas Chasma basin (Fig. 1a), and hosts a perched basin that contains drainage valleys and fan-delta complexes. Bright mounds and layered strata are also found within the center of the basin. Previous studies have identified clear evidence of polyphase fluvial activity in Southwest Melas as well as the presence of silica in a few light-toned outcrops throughout the basin [1,2,3], However, the formation mechanisms of these silica-bearing features remain poorly constrained. In this study, we use hyperspectral orbital data and high-resolution images to constrain the origins of various silica-bearing morphologic features in Mars' Southwest Melas Chasma as well as determine whether or not some features are the result of subaqueous hydrothermal activity, which would help to constrain the basin's biosignature preservation potential.

Methods: To analyze the morphologic aspects of various features of Southwest Melas, we used imagery from the High-Resolution Imaging Science Experiment (HiRISE) as well as the Context Camera (CTX) onboard the Mars Reconnaissance Orbiter (MRO) [4,5]. For spectral analysis, we used visible/near-infrared (~0.3–2.6 μm) hyperspectral data from the MRO's Compact Reconnaissance Imaging Spectrometer for Mars (CRISM). The CRISM images used were all acquired at the most recent calibration level (MTRDR - Mapped Targeted Reduced Data Record; [6]). These images have been processed to suppress atmospheric and instrumental effects [6], but still require ratioing with spectrally neutral terrains to bring out subtle spectral features. All of the MTRDR images were downloaded with a set of pre-calculated spectral parameter maps, derived from I/F cubes and refined to reduce spectral noise [7]. These spectral parameter images were used to generate RGB composites (Fig. 1b) to evaluate spectral diversity of the overall region.

Results (Morphology): One of the main morphological features observed were light-toned raised plateaus or "mounds". These mounds varied in size and topography and all exhibited an irregular shape. The mounds are concentrated in the center of the basin, in areas identified as the original lacustrine sediment deposits [3]. The mounds are commonly steep-sided, ranging in height from 10-20 m, and typically carry irregular depressions exposing internal layers on their top surface. We selected 14 mounds for study and named them with letters in order of decreasing perimeter size, Mound A being the largest. The main mound studied was Mound B (Fig. 1c), an oblong mound about 12 m tall, 500 m long, and 450 m wide at its widest point. 3D imagery of the mound using HiRISE data shows the significant elevation changes on the eastern half of the mound, displaying a central pit and/or dip on the southwestern part of the mound, as well as terrace-like features around the raised portions of the mound.

We also identified light-toned "patches" with rubbly textures. While the mound features are all raised above the surrounding surface, these patch features are flush with the surrounding surface and not elevated.

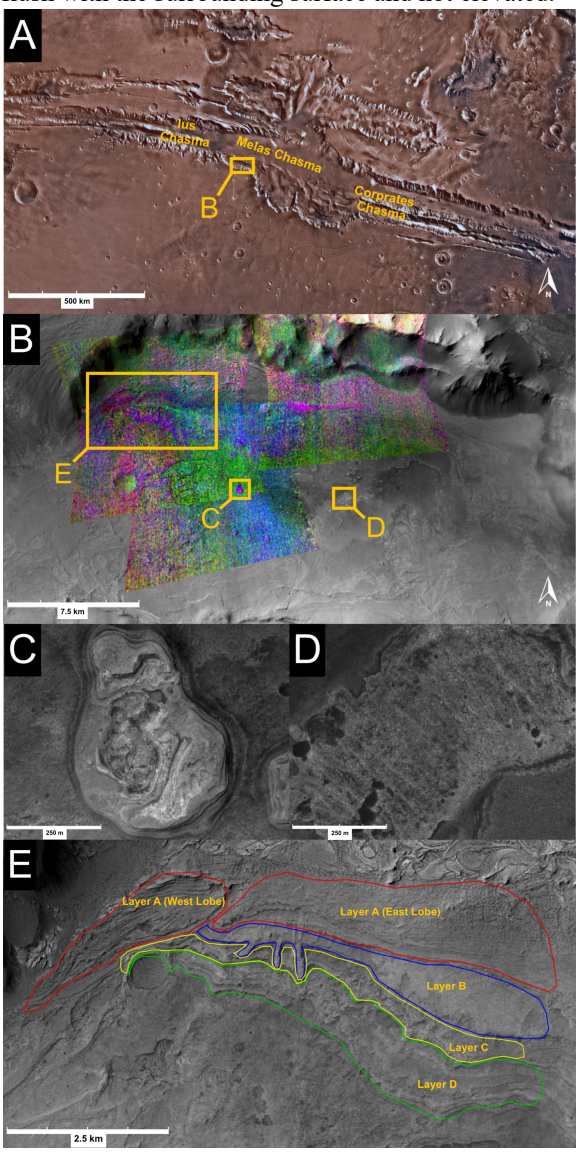

Figure 1: *(a) Location of Southwest Melas study area within Valles Marineris. (b) CRISM RGB parameter combination (SINDEX2/BD2100_2/BD1900_2) overlaid on a CTX map of our study area. HiRISE images of (c) Mound B, (d) Patch A, and (e) the spectrally diverse layered strata.*

Otherwise, the patches seem to have similar properties to the mounds. They have a similar scaly/rubbly texture, and boulders ~5m in diameter. We identified eight patches in the same vicinity of the mounds and named them using the same format. The main patch studied was Patch A (Fig. 1d), due to it being the most prominent in both size and in spectral contrast (Fig. 2). Patch A is oblong-shaped, 850 m long and 400 m wide. It has alternating ridges of high and low albedo, with dark spots of fine-grained material. It also has a well-defined outer boundary despite lacking significant elevation.

The mounds and patches are superposed on layered strata, which are best exposed in the northwest corner of the basin (Fig. 1e). We catagorized the layers based on stratigraphic relationship, textural morphology, and spectral contrast within the spectral summary parameter combination in Fig 1b. The layers at this location exhibit a scaly/rubbly texture, similar to that of the patches and mounds. Some areas, however, have a more honeycomb texture, or are covered in fine-grained material. The layers are broken up at larger scales than the patches and mounds, creating a rough surface broken into boulders 5-15 m in diameter.

Results (Spectral): A few of the mound features exhibit spectral properties distinct from the surrounding material (Fig. 1b) and consistent with hydrated silica. Mound B stood out among the rest, containing relatively clear absorption bands at 1.9, and 2.2 μm in its ratioed spectra (Fig. 2a). These features appear most consistent with that of Opal-A lab spectra (Fig. 2b), however, the ratioed spectra lack a strong 1.4 μm absorption. This could be the result of dust and other surface debris interfering with the spectra and weakening the absorption feature. A few patches showed similar spectral properties as the mounds, with the standout location being Patch A, which also lacked a strong 1.4 μm absorption, likely due to similar causes affecting Mound B. The layers displayed significant spectral diversity, both from strata to strata, and even within single strata. The northernmost layer, Layer A, contained two lobes, a west lobe and an east lobe. Spectral parameter maps over Layer A suggested hydrated silica and polyhydrated sulfates throughout the layer, and spectra from both lobes of Layer A are consistent with jarosite (bands near 0.9 and 2.26 μm). Layer C exhibited signatures of hydrated minerals, monohydrated sulfates, pyroxene, and possible patches of opal in parameter maps. Spectrally, Layer C had a similar absorption band to Layer A around 2.2 μm, consistent with hydrated silica. Layers B and D contained signatures of polyhydrated sulfates, hydrated minerals, and pyroxenes within the parameter maps, but exhibited no clear absorption bands in extracted spectra.

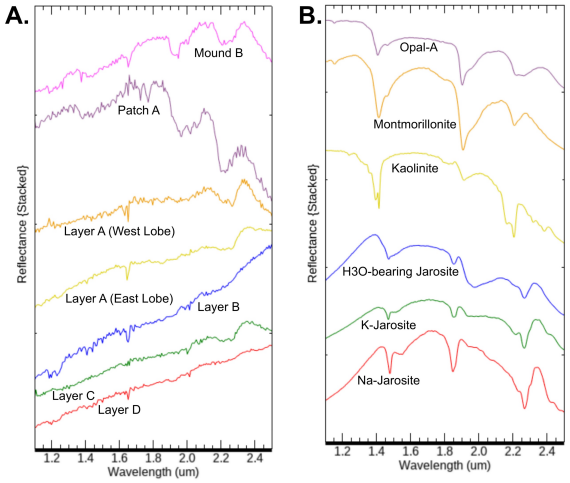

Figure 2: *(a) Unsmoothed ratioed CRISM spectra taken from features in Melas compared to (b) lab spectra.*

Discussion: We have identified silica in the mounds, patches, and in some lacustrine sedimentary layers in Southwest Melas basin. The mounds are morphologically similar to hydrothermal spring mounds on Earth, which are also commonly dominated by hydrated silica [8,9]. The patches bear similar resemblance and spectral features to the mounds, therefore, we believe they were formed by hydrothermal activity, but have a different surface expression perhaps either because they are also subaerial mounds that have not been eroded to form resistant mounds or because they formed under different conditions. Subaqueous flows would be expected to spread out much more than subaerial flows [8], which could be consistent with the lack of topographic relief of the patches. Indeed, the detection of silica in the northwest sedimentary layers suggest interplay between lacustrine and hydrothermal activity. Subaqueous hydrothermal activity would affect the lake chemistry, possibly producing sulfates and silica deposits in the layers [10]. The base of Mound B also sits in the same stratigraphic level of a few fans which have been identified as identified as deep sub-lacustrine in origin [1]. Lacustrine hydrothermal systems support significant biomass and can entomb microorganisms in spring deposits or cemented sediments, making Southwest Melas a potential hotspot of biosignature preservation [10].

References: [1] Williams and Weitz (2014) *Icarus, 242,* 19-37. [2] Weitz et al. (2010) *Icarus, 205,* 73-102. [3] Davis et al. (2018) *JGR, 123,* 2527–2549. [4] McEwen et al. (2007) *JGR, 112,* E05S02. [5] Malin et al. (2007) *JGR, 112,* E05S04. [6] Seelos et al. (2016) *LPI, 1903,* 1783. [7] Viviano-Beck et al. (2014) *JGR, 119(6),* 1403-1431. [8] Jones et al. (2007) *Journal of the Geological Society, London, 164,* 227–242. [9] Ruff et al. (2020) *Astrobiology, 20,* 475–499. [10] Sugitani et al. (2015) *Geobiology, 13,* 522-545.